David M. Gullotti
Department of Bioengineering,
University of Pennsylvania,
240 Skirkanich Hall,
210 S. 33rd Street,
Philadelphia, PA 19104-6321

Matthew Beamer
Department of Bioengineering,
University of Pennsylvania,
240 Skirkanich Hall,
210 S. 33rd Street,
Philadelphia, PA 19104-6321

Matthew B. Panzer
Department of Biomedical Engineering,
Duke University,
Durham, NC 27708

Yung Chia Chen
Department of Bioengineering,
University of Pennsylvania,
240 Skirkanich Hall,
210 S. 33rd Street,
Philadelphia, PA 19104-6321

Tapan P. Patel
Department of Bioengineering,
University of Pennsylvania,
240 Skirkanich Hall,
210 S. 33rd Street,
Philadelphia, PA 19104-6321

Allen Yu
Department of Biomedical Engineering,
Duke University,
Durham, NC 27708

Nicolas Jaumard
Department of Bioengineering,
University of Pennsylvania,
240 Skirkanich Hall,
210 S. 33rd Street,
Philadelphia, PA 19104-6321

Beth Winkelstein
Department of Bioengineering,
University of Pennsylvania,
240 Skirkanich Hall,
210 S. 33rd Street,
Philadelphia, PA 19104-6321;
Department of Neurosurgery,
University of Pennsylvania,
Philadelphia, PA 19104

Cameron R. Bass
Department of Biomedical Engineering,
Duke University,
Durham, NC 27708

Barclay Morrison
Department of Biomedical Engineering,
Columbia University,
New York, NY 10027

David F. Meaney[1]
Department of Bioengineering,
University of Pennsylvania,
240 Skirkanich Hall,
210 S. 33rd Street,
Philadelphia, PA 19104-6321;
Department of Neurosurgery,
University of Pennsylvania,
Philadelphia, PA 19104

Significant Head Accelerations Can Influence Immediate Neurological Impairments in a Murine Model of Blast-Induced Traumatic Brain Injury

*Although blast-induced traumatic brain injury (bTBI) is well recognized for its significance in the military population, the unique mechanisms of primary bTBI remain undefined. Animate models of primary bTBI are critical for determining these potentially unique mechanisms, but the biomechanical characteristics of many bTBI models are poorly understood. In this study, we examine some common shock tube configurations used to study blast-induced brain injury in the laboratory and define the optimal configuration to minimize the effect of torso overpressure and blast-induced head accelerations. Pressure transducers indicated that a customized animal holder successfully reduced peak torso overpressures to safe levels across all tested configurations. However, high speed video imaging acquired during the blast showed significant head accelerations occurred when animals were oriented perpendicular to the shock tube axis. These findings of complex head motions during blast are similar to previous reports [Goldstein et al., 2012, "Chronic Traumatic Encephalopathy in Blast-Exposed Military Veterans and a Blast Neurotrauma Mouse Model," Sci. Transl. Med., **4**(134), 134ra160; Sundaramurthy et al., 2012, "Blast-Induced Biomechanical Loading of the Rat: An Experimental and Anatomically Accurate Computational Blast Injury Model," J. Neurotrauma, **29**(13), pp. 2352–2364; Svetlov et al., 2010, "Morphologic and Biochemical Characterization of Brain Injury in a Model of Controlled Blast Overpressure Exposure," J. Trauma, **69**(4), pp. 795–804]. Under the same blast input conditions, minimizing head acceleration led to a corresponding elimination of righting time deficits. However, we could still achieve righting time deficits under minimal acceleration conditions by significantly increasing the peak blast overpressure. Together, these data show the importance of characterizing the effect of blast overpressure on head kinematics, with the goal of producing models focused on understanding the effects of blast overpressure on the brain without the complicating factor of superimposed head accelerations.* [DOI: 10.1115/1.4027873]

Keywords: blast, traumatic brain injury, biomechanics, acceleration, overpressure

[1]Corresponding author.
Manuscript received June 21, 2013; final manuscript received June 11, 2014; accepted manuscript posted June 19, 2014; published online July 10, 2014. Assoc. Editor: Brian D. Stemper.

Introduction

Blast-induced traumatic brain injury (bTBI) is a well-recognized injury occurring in the modern military environment [1,2], and determining bTBI etiology is a major focus across many laboratories. Some contributing mechanisms for bTBI are shared with mechanisms for traumatic brain injuries in the civilian population, because some phases of bTBI include contact and inertial loading (acceleration) mechanisms [3]. However, it is not yet clear if there are *unique* mechanisms associated with *primary* blast loading that contribute to the resulting neurological impairment of bTBI.

Animate models are critical for revealing potentially new mechanisms of primary blast injury. Although some studies use explosive charges to produce a blast wave, a more common method uses a shock tube to deliver repeatable, precise shock waves that mimic the free field pressures measured during explosion events [4]. These reduced models of blast loading often protect much of the organism from the blast loading and therefore do not fully replicate the exposure to the entire body that would occur in combat. Nevertheless, these reduced models allow one to focus specifically on the mechanisms of injury and brain tolerance to blast loading. Considerable past work in the development and characterization of shock tube designs now provides several options to study the effect of blast waves in rodents [3,5–11]. Moreover, additional shock tube designs are used to study blast loading in larger animals as well as in vitro preparations [12–14]. Many new designs offer methods to control or minimize pulmonary trauma from the blast wave loading, as pulmonary injury can complicate the blast-induced brain pathology. Less understood in these bTBI models are the key methodological variables that can influence the resulting biomechanical characteristics of the injury. Recent efforts are beginning to better describe the relationship between the magnitude, direction, and duration of the external shock wave to the resulting complex intracranial pressures that can be generated within the brain parenchyma as the shock wave transits through the brain [14–18]. Additional studies show how the complex characteristics of the blast exposure, which often includes both a blast wave and blast wind event, leads to significant head motions and skull deformation [5,19,20]. Moving the animal outside the path of the blast wind significantly affects head motion, but this change in head motion was only recently measured [11,21].

This paper presents a biomechanical characterization of a common configuration used in a shock tube-based model of blast TBI in the mouse. We specifically chose a system where we isolated the effects of the blast exposure on the head by protecting the remainder of the body during the blast. We identify key methodological features that contribute to the type and severity of injury in the mouse, measure the relative motion of the mouse head during a blast event in three different test configurations, and evaluate if this model is capable of creating immediate neurological impairment. We report that significant head motions and accelerations can occur when studying blast exposure using a shock tube device. Finally, we show that restraining head motion and changing orientation significantly influence the survivability and immediate neurological impairment following exposure to the shock wave. These data highlight that shock tube-based rodent models must be developed carefully to avoid inertial (acceleration) effects to the brain. Without a systematic evaluation of the model biomechanics, it is not assured that a shock tube-based model will apply solely to primary blast TBI.

Materials and Methods

Shock Tube Design. We used three main criteria in the shock tube development. First, we manufactured the tube from commercially available components, providing a template for other research groups to easily reproduce the design. Second, we adjusted the volume of the chamber to shape the characteristics of the input wave; these include the duration, onset, and decay of the blast input. We used a chamber volume in the driver section of 238.9 cm^3 (78 mm diameter, 50 mm long), followed by a 1240 mm long, 78 mm diameter section of aluminum tubing positioned after the membranes. Third, we used Mylar membranes, commercially available in several thicknesses (McMaster Carr (MMC), Cleveland, OH), as the material that ruptures to initiate the shock wave. The shock tube design, developed in detail in a separate publication [3], used helium as the gas for the driver section and a set of gas solenoids to control both the filling and exhaust of the driver section.

Mouse Holder Design. In some past configurations, the animal is placed immediately outside the tube, permitting the investigator to visually observe the animal status prior to and immediately following blast exposure. We studied the configuration of the animal outside the tube in more depth, since preliminary testing showed that inserting the animal into the tube would create very complex blast wave characteristics at the head surface. The primary disadvantage of this approach is that the blast loading is composed of a rapid onset shock wave and a subsequent blast wind that complicates the study of the biomechanical loading experienced by the head. Moreover, we used an animal holder that would position the center of the mouse head at a prescribed distance (15 mm) from the exit of the tube where the shock wave is still nearly planar [22], as well as different radial distances from the tube's centerline axis to examine the reproducibility, distance dependence, and potential complication factors with animal misalignment. A disadvantage of this method is that the induced head motion from blast exposure will vary with the direction of the applied blast loading—e.g., applying the blast exposure to the lateral head surface would lead to more motion that a blast wave directed toward the dorsal head surface, since the animal was laid prone on the animal holder surface. A stock, threaded aluminum tube (Part No. 44705K233, MMC) was cut to length (15 cm), inserted into a threaded flange (Part No. 4568K273, MMC) and filled with a urethane material to provide a flat surface for mounting the mouse in a prone position. Resting on a thin trapezoidal extension of the holder, the head was exposed to the shockwave while the rest of

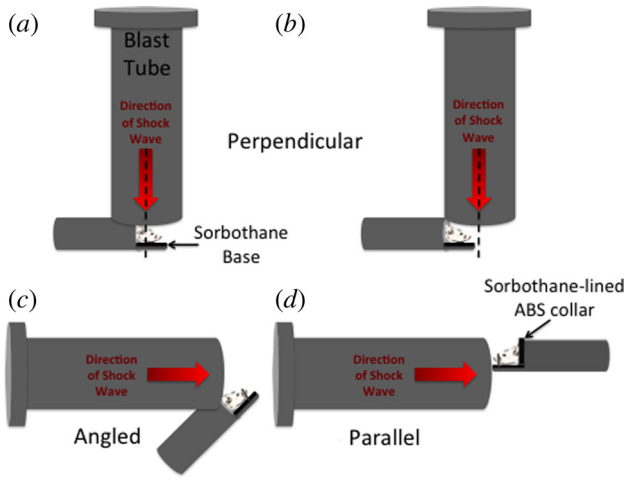

Fig. 1 Diagrams representing the different animal orientations relative to the blast tube. All orientations held the distance from the exit of the tube to the center of the mouse head constant. (*a*) Perpendicular orientation with the center of the mouse head aligned with the center of the tube's axis. The location of the Sorbothane base indicated is consistent in all orientations. (*b*) The same perpendicular orientation used in (*a*) with the mouse's head aligned with the inner periphery of the tube. (*c*) Angled orientation with the mouse head aligned with the inner periphery of the tube. (*d*) Parallel orientation with the mouse head constrained by a Sorbothane-lined collar.

the body was encased by the aluminum tube. The interior surfaces of the holder were lined with a blast absorbing material (Sorbothane, Part No. 8514K362, MMC), and the animal was secured in place to minimize any indirect transfer of the blast wave along the animal torso. In two of our configurations (angled and parallel; Figs. 1(*c*) and 1(*d*)), a thin metal rod was positioned on the holder to secure the snout and limit the lateral motion of the head. Extensive snout damage occurred if this thin metal rod was used in the vertical configuration, and therefore the perpendicular tests had no snout constraint.

Collar Design. In some experiments, we exposed the mouse to a shockwave traveling parallel to its body's long-axis. To restrain head motion, we designed a custom cervical collar made of Sorbothane that allowed normal ventilation. The design was wedge-shaped to accommodate variation in the anatomy of different test subjects. The position of the collar relative to the mouse was adjustable to ensure a secure fit for each mouse. We also used a thin metal bar to position and point the snout directly into the shock tube. Finally, the top surface of the animal holder was replaced with clear polyethylene terepthalate (PETG) tubing (Part No. 9245k51, MMC) to visualize the torso and verify that collar positioning did not obstruct breathing.

Animal Orientation. Animals were oriented in one of three different positions relative to the direction of blast wave propagation (Fig. 1): (1) **perpendicular** to the blast wave exiting from the shock tube, with the head center either (a) aligned with the center of the tube axis or (b) aligned within the inner periphery of the shock tube, (2) **angled** 45 deg from the shock tube axis with the nose pointing away from the tube exit, and (3) **parallel** to the axis of the shock tube with the nose pointing toward the tube exit.

Pressure Recording. We used pressure transducers with sufficient dynamic frequency response (Endevco, model 8530B-200, San Juan Capistrano, CA) to record the pressure at the exit of the shock tube. We used three equally spaced transducers along the perimeter of the blast tube to evaluate wave symmetry and acquired pressure data using a MATLAB-based data acquisition program sampling at 200 kHz per channel. These pressure transducers were located 21 mm along the shock tube axis from the animal head. We placed a fourth pressure transducer within the animal holder cavity, located in an area adjacent to the animal torso, to assess the potential indirect transfer of any blast wave along its axis. To eliminate aliasing artifact, we conditioned each pressure transducer signal with an inline filter conditioning box (Alligator Technologies, USBPGF-S1, Costa Mesa, CA) set to provide a 20 kHz cutoff frequency linear phase filter.

Shock Tube Characterization. Shock tube designs often create a rapid onset shock wave that is followed by a longer duration pressure decay. In many designs, the pressure loading is complicated by the blast wind following the shock wavefront. We measured the profile of the shockwave within the length of the tube and in the immediate vicinity of the shock tube exit. To assess the relative level of the blast wind at different locations, we inserted elastic cylinders that extended 12 mm into the tube cross section from the tube wall. As the blast wind traveled across the cylinder, the insert would deflect in response to the applied dynamic pressure. We used high speed video to record the dynamic deflection of the elastic cylinders at different points along the tube length as the blast wind passed across the elastic cylinder. We used the same configuration of elastic cylinders to measure the relative effect of the blast wind at different points from the exit of the shock tube.

High Speed Video. We used a high speed video acquisition system (Phantom v4.2 camera, Vision Research, Wayne, NJ) to record head motion either from the side or front of the blast tube, corresponding to a lateral or frontal view of the animal head. For all reported tests, the framing rate was set to either 10 kHz (resolution: 256×128; $N = 1$) or 22 kHz (resolution: 128×128; $N = 17$). Fiducial markers in the field of view provided a calibration measure for lengths and displacements in the x and y (frontal view) or y and z (lateral view) direction.

A MATLAB-based image processing algorithm was used to manually track the fiducial markers on the head during the blast sequence. The position of the eye in the field of view was used as a surrogate marker for head movement. The two fiducial markers defined in the tracking algorithm were used to measure the movement of the head center during blast. We tracked both the displacement vector and the x and y displacement components over the entire duration of the experiment that included a pretriggering period (5 ms) and the movement for the first 30 ms during and following the blast event, since preliminary testing showed negligible head movement after that timepoint. We used data smoothing algorithms (zero-phase 8th order Butterworth filter, 1 kHz cutoff frequency for vertical (y-axis) data and 6th order, 500 Hz cutoff frequency for horizontal (x-axis) data) on the tracked displacement data. The filter cutoff frequencies were selected to ensure that the root mean squared residual displacement calculated between the original and filtered data varied less than 0.5% over the sampling interval. We next applied a first order Euler's approximation to calculate the velocity and, in turn, the acceleration in the x-y or y-z laboratory coordinate system based on these displacement data. Similar to displacement, we calculated the resultant magnitude, as well as the x and y components, of the velocity and acceleration.

Animal Preparation and Injury. Male, C57BL6 mice aged 12–14 weeks were obtained from either Charles River laboratories (Wilmington, MA) or Taconic (Hudson, NY) and allowed to acclimate in the colony before testing. We carefully adhered to the animal welfare guidelines established by the University of Pennsylvania's and Columbia University's Institutional Animal Care and Use Committee (IACUC) and used procedures that were approved by those IACUCs. Animals used to characterize the head motion during blast were euthanized immediately prior to placement in the animal holder. All animals were tested within 40 min of euthanization to minimize the influence of changes in tissue properties due to rigor mortis. A limited series of tests comparing the response of freshly euthanized mice to anesthetized mice showed that there was no significant difference in the head trajectories following blast exposure. In separate tests to measure the neurological impairments after blast exposure, animals were placed in an anesthesia induction chamber (5% isoflurane) for 2 min, and then transported into the testing room. Animals remained on 2% isoflurane anesthesia for 3 min during placement and positioning prior to exposure. Immediately prior to testing, anesthesia was discontinued. Immediately after injury, the animal was removed from the holder and brought to a recovery area.

Survival curves for the three different loading conditions were generated using logistic regression techniques. An approximately equal number of animals exposed to blast either survived (0) or died (1) within 5 min after the exposure. A range of blast pressures were used to develop a group of animals spanned both survivable and fatal blast exposures. Data for each group were analyzed using logistic regression techniques to determine a 50% survivability exposure level.

For animals surviving a blast exposure, neurological impairment immediately after blast was measured using a righting time response, a common early measure of impairment used in models of traumatic brain injury to assess an initial neurological deficit [21,23–25]. To measure righting time, we placed the mouse on its back and measured the time elapsed until it turned over and righted onto all four paws. Recording time started when the animal was removed from the animal holder following blast or sham exposure. Once animals regained the ability to right themselves, they were

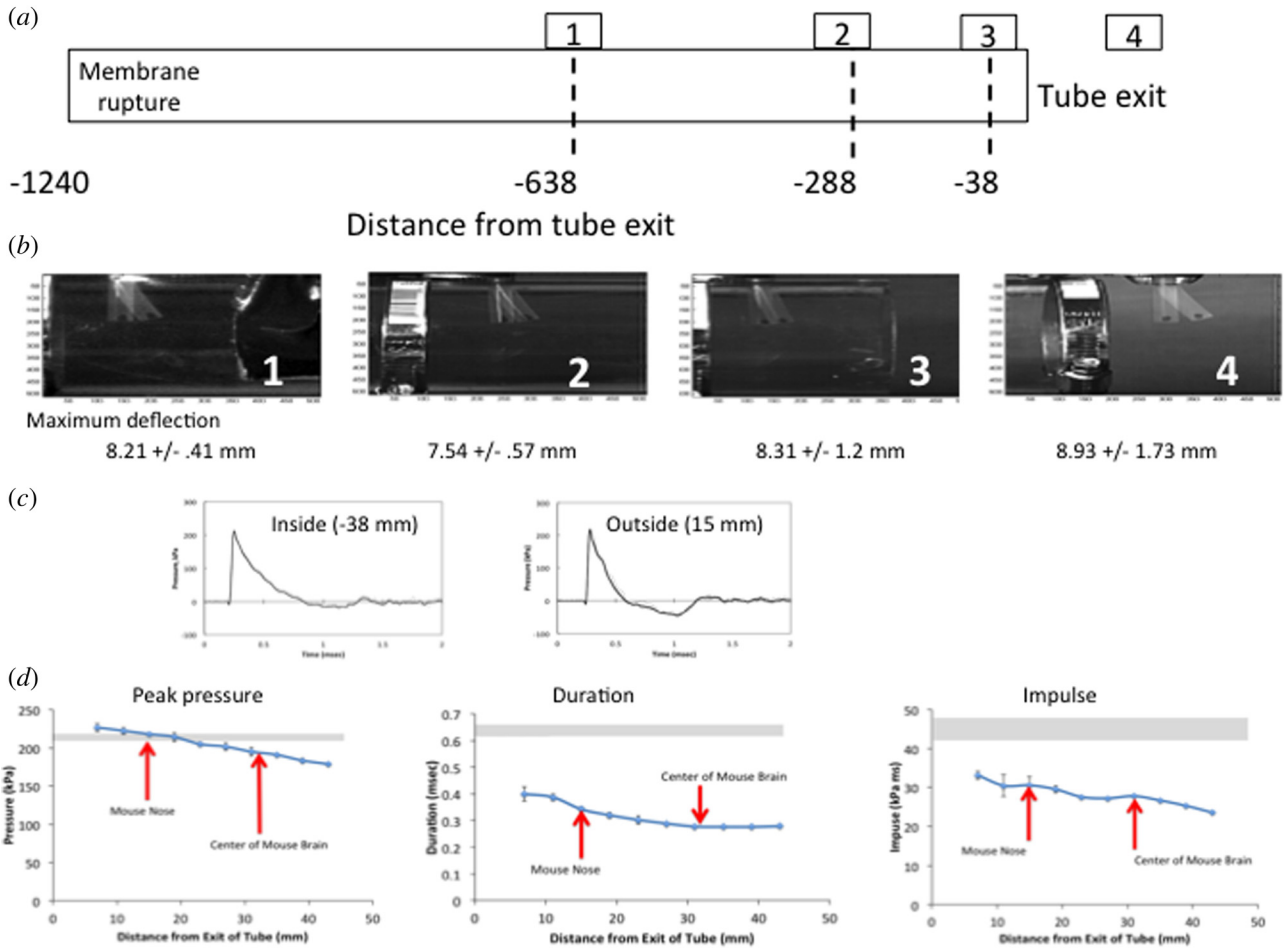

Fig. 2 Shock tube characterization. Pressure transducers located along different points within and outside the tube (*a*) were used to measure the static pressure during a blast event. For measures outside the tube, the transducers were located at the same radial location as the tube wall. Additionally, small elastic cylinders were inserted into the path of the blast waves, extending slightly from the tube wall. The blast wind traveling across these elastic cylinders caused the cylinder to deflect ((*b*), shown for regions outlined in (*a*)). The magnitude of the peak displacement of the tip is shown for each region; no significant difference in deflection occurred across the four observation points. (*c*) Measures of pressure within (−38 mm) and outside (+15 mm) showed a slight attenuation of the peak pressure and a more dramatic reduction in the duration. (*d*) Across the distances beyond the tube exit that contained the animal head, there was significant differences to the peak pressure, duration, and impulse (grayed regions in each plot denote range (mean ± SD) of pressure profile characteristics within the tube.).

monitored for several minutes while they established their movement and exploratory behavior before they were returned to a warmed recovery cage and monitored for future status.

Statistical Analyses. We used an analysis of variance (ANOVA) model to compare peak velocities and accelerations across different testing configurations. We used Student's t testing to compare pressure data as well as righting times between sham and injured animals in each testing configuration. Unless otherwise noted, all data are reported as mean ± standard deviation (SD). For all tests, significance was set at $p < 0.05$.

Results

Free field blast events show a characteristic rapid increase in pressure that corresponds with the initial arrival of the shock wavefront, followed by a rapid, exponential decay that can include a modest negative pressure [26]. Our design successfully recreated the sharp rise and rapid decay, but did not include the significant negative pressure phase commonly found with large explosions (Fig. 2). This blast waveform was repeatable for test conditions that spanned peak pressures of 120–500 kPa (Table 1). Peak overpressures around the perimeter of the tube varied less than 15% within individual tests and less than 7% across tests using the same membrane thickness.

Within the shock tube, the peak pressure and duration of the pressure did not vary significantly along the length of the tube (ANOVA; $p = 0.48$). We compared pressure profiles just within the tube exit (−6 mm) and just beyond the tube exit (+31 mm)

Table 1 Average values and SDs collected at the exit of the blast tube from shock waves created from rupturing various thicknesses of polyethylene (PET) membranes. Each value represents the average across all three transducers from four consecutive tests

Membrane thickness (in.)	Peak overpressure (kPa)	Duration (ms)	Impulse (kPa · ms)
0.010	139 ± 5	0.39 ± 0.04	18 ± 2
0.020	215 ± 13	0.65 ± 0.04	46 ± 5
0.030	275 ± 24	0.80 ± 0.03	77 ± 7
0.040	329 ± 31	0.91 ± 0.05	106 ± 9
0.050	390 ± 24	0.98 ± 0.04	135 ± 11
0.055	415 ± 41	1.02 ± 0.04	148 ± 12
0.060	448 ± 29	1.07 ± 0.02	163 ± 12

(Figs. 2(*c*) and 2(*d*)). The position outside the tube corresponded to the approximate center of the mouse head. We observed a significant decrease in the duration (0.28 ± 0.003 ms (outside) versus 0.636 ± 0.016 ms (inside), $p < 0.05$; Student's t test) and pressure magnitude (212.3 ± 4.5 kPa (outside) versus 194.98 ± 5.55 kPa (outside) kPa; $p < 0.05$; Student's t test). Together these led to a significant reduction in the impulse between these two positions (46.6 ± 1.4 kPa·ms (inside) versus 27.8 ± 0.31 kPa·ms; Fig. 2(*d*)). In comparison, we observed no difference in the peak displacement of an elastic cylinder extended radially into the shock tube (Figs. 2(*a*) and 2(*b*)).

With the animal holder positioned in the centered perpendicular orientation at the blast exit, we observed a consistent secondary reflected pressure spike recorded for each test (0.508 mm membrane thickness; Fig. 3(*b*)). Due to this wave reflection, the magnitude of the peak pressure averaged across all three transducers was significantly larger ($p < 0.01$; Student's t test) with the animal holder in place (259 ± 15 kPa) when compared to tests in which the holder was not used (215 ± 13 kPa). Readings from the pressure sensor located most distant from the animal holder (sensor 1) did not differ from free field pressures ((229 ± 16 kPa (with holder) versus (227 ± 4 kPa (free field); $p = 0.57$; Student's t test), while the second and third pressure sensors closest to the animal holder (sensor 2 and sensor 3) displayed higher peak pressures (292 ± 19 kPa (sensor 2) and 257 ± 20 kPa (sensor 3)) that were significantly different ($p < 0.01$; Student's t test) from the free

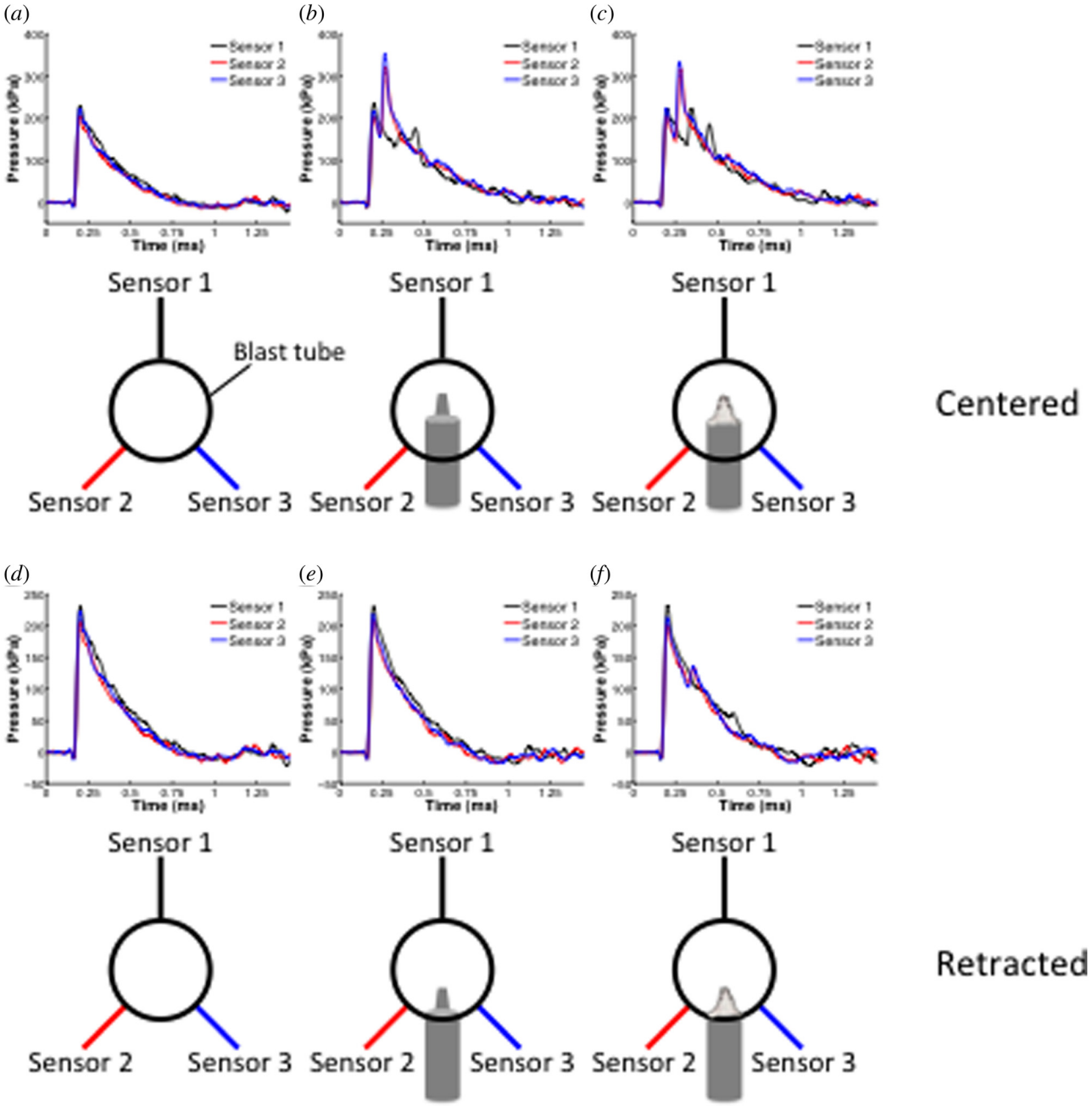

Fig. 3 Representative pressure traces gathered from the three sensors at the exit of the blast tube with the mouse holder in different positions. All tests were conducted in the perpendicular orientation. Under each trace is a top view of the corresponding animal holder position relative to the blast tube. Both centered ((*a*)–(*c*)) and retracted ((*d*)–(*f*)) positions were tested without obstruction, with only the mouse holder, and with both the holder and mouse present. Traces are color coded to match the corresponding diagrams.

field pressure for each sensor position (201 ± 3 kPa (sensor 2) and 218 ± 6 kPa (sensor 3)). In comparison to the pressure transducer measurements along the perimeter of the shock tube exit, the pressure transducer recordings within the animal holder tube without an animal inside were significantly less (219 ± 15 kPa (average across perimeter sensors) versus (156 ± 8 kPa (within holder); $p < 0.01$; Student's t test).

Positioning an animal within the holder assembly led to no differences in peak pressures for all three transducers located at the blast tube exit when compared to pressures recorded with only the animal holder in place (Fig. 3(*c*)). Although peak pressure was not significantly affected, the presence of the animal's head led to a small transient increase in pressure during the decay phase of the waveform measured by sensor 1. We observed a significant reduction in the pressure measured at the approximate torso location when an animal was placed in the assembly (156 ± 8 kPa (empty holder) versus 12 ± 3 kPa (animal in position); $p < 0.01$; Student's t test). In all tests, peak torso pressure was well below the threshold pressure associated with pulmonary trauma [27].

These data show that placing the animal holder in the blast wave path creates a more complex blast loading profile. We next tested if we could adjust the position of the animal holder at the exit of the shock tube to minimize the effect of the holder. Placing the holder near the periphery of the shock tube (Fig. 3(*e*)) substantially reduced reflections of the shockwave, and the measured peak pressures averaged across the sensors (224 ± 10 kPa) were not significantly different from the peak pressures measured in the free field condition (215 ± 13 kPa) ($p = 0.26$; Student's t test).

These tests confirmed it was possible to place the animal holder at the exit of the blast tube and minimally interfere with the input blast wave. We next tested if the position of the mouse at the tube exit significantly influenced the head motion occurring during the blast event. When the head was oriented perpendicular to the blast wave (Fig. 1(*b*)), it showed three general phases of motion during the blast event: a rapid, nearly vertical downward motion, followed by a slightly longer upward motion, and then a slowly tracking lateral motion as the head rotated and slowed into its near final position (Figs. 4(*a*) and 4(*b*)). Starting from its rest position, trials across different test animals showed a relatively consistent peak downward displacement (Fig. 4(*b*)). When the animal was placed at an angle of 45 deg to the direction of the shock wave, video footage revealed significant flexion movement of the animal head into the supporting Sorbothane layer, followed by an extension of the head beyond the initial position (Figs. 4(*c*) and 4(*d*)). When the animal was placed parallel to the direction of the shockwave, we supported the occiput with a custom-designed cervical collar. In this configuration, very minimal head displacement was observed (Figs. 4(*e*) and 4(*f*)).

Across the three positions studied (Figs. 1(*b*), 1(*c*), and 1(*d*)), we used the displacement data to determine if there were significant differences in the accelerations occurring across these tests. Figures 5(*a*)–5(*f*) present representative illustrations of the filtering process, as well as velocity and acceleration traces for the perpendicular configuration. In the perpendicular configuration, peak vertical accelerations ($a_y = 15{,}900 \pm 5400\ \text{m/s}^2$) were significantly larger than peak lateral accelerations ($a_x = 870 \pm 470\ \text{m/s}^2$; $p < 0.01$; Student's t test). We did not see a significant difference in the head kinematics between anesthetized, living mice, and freshly euthanized mice (Fig. 5(*g*)). In the angled configuration, the vertical head acceleration magnitude (a_y) was significantly less than the perpendicular configuration ($3960 \pm 970\ \text{m/s}^2$ (angled) versus $15{,}900 \pm 5400\ \text{m/s}^2$ (perpendicular); $p < 0.01$; Student's t test). The parallel configuration produced peak vertical accelerations that were comparable to those of the angled orientation, but significantly smaller than in the perpendicular orientation, and peak horizontal accelerations that were significantly smaller than in both the perpendicular and angled configurations ($a_y = 3940 \pm 1210\ \text{m/s}^2$; $a_z = 1240 \pm 110\ \text{m/s}^2$; $p < 0.01$, Student's t test). Both the angled and parallel orientations produced significantly lower peak resultant accelerations than the perpendicular orientation ($5320 \pm 620\ \text{m/s}^2$ (angled) and 4110 ± 1180 (parallel) versus $16{,}830 \pm 5720\ \text{m/s}^2$ (perpendicular); $p < 0.05$; Student's t test, Fig. 5(*h*)).

These tests demonstrated that it was possible to develop a blast testing protocol to examine two different biomechanical scenarios: (1) a blast wave transmitting a significant head acceleration (perpendicular orientation, Fig. 1(*b*)), and (2) a blast wave with minimal head acceleration (parallel orientation, Fig. 1(*d*)). We explored the effect of these two kinematic scenarios by measuring the survivability and threshold for neurological impairment in these conditions. We defined fatalities as death that occurred within 5 min of blast exposure, and we generated an approximately equal number of surviving and fatal cases of blast exposure in each condition to generate a logistic regression curve (perpendicular—9 fatal, 12 survived; angled—7 fatal, 9 survived; parallel—8 fatal, 13 survived). We found that the perpendicular orientation—with significant head acceleration—showed a significantly lower 50% survival threshold in mice when compared to the parallel orientation (246 ± 4 kPa (perpendicular) versus 405 ± 10 kPa (parallel); Fig. 6(*a*); $p < 0.01$; Student's t test). These thresholds were also significantly different when the impulse loading was used, to reflect both the peak and duration of applied pressure ($114.1 + 1.9$ kPa·ms (perpendicular) versus $286.7 + 7.1$ kPa·ms (parallel); Fig. 6(*b*); $p < 0.01$; Student's t test). Similarly, for the same blast input (0.508 mm membrane thickness; 215 ± 13 kPa), we observed that significantly reducing the head acceleration (parallel configuration) led to a significant reduction in righting time (307 ± 74 s (perpendicular) versus 60 ± 5 s (parallel); Fig. 5(*c*); $p < 0.01$; Student's t test). Finally, we tested if pressure alone—with no significant acceleration—could alter neurological impairment. Using the survival dataset as a guide, we found a blast overpressure level (415 ± 41 kPa) in the parallel configuration that produces a significant alteration in the righting time reflex immediately after exposure relative to sham ($p < 0.01$; Student's t test; Fig. 6(*c*)). Across all tests, none of the animals exposed to blast loading showed macroscopic signs of pulmonary trauma (Fig. 6(*d*)) and no obvious change in respiration rate. We observed no signs of subarachnoid hemorrhage, brainstem lesions, or subdural bleeding (Fig. 7) in animals surviving the blast exposure. Animals not surviving the blast exposure often showed small areas of hemorrhage in the lower brainstem region. None of the animals showed signs of macroscopic lung injury following any of the applied loading conditions (Fig. 7). Moreover, all surviving animals were ambulatory by 1 day following injury, appearing only slightly lethargic with less active exploratory behavior compared to sham mice. Normal grooming behavior recovered within 2–3 days post injury.

Discussion

We report a model of blast-induced TBI in the mouse and concentrate on defining the biomechanical characteristics of this model. We show it is possible to reproducibly create a Friedlander-type blast wave with a shock tube design that is portable and requires minimal laboratory space. In addition, we found that blast loading can cause significant head accelerations in the mouse. The relative amount of induced head acceleration was controlled by changing the orientation of the animal to the blast wave and by providing a simple snout restraint system for the head during the blast. In turn, the threshold for survivability to the blast exposure was negatively influenced by the presence of significant head accelerations; removing these head accelerations and changing the orientation of the incoming blast wave increased the survivability threshold by more than 60%. Similarly, we found immediate neurological impairment as measured by righting time after blast exposure that was strongly influenced by the magnitude of head acceleration; minimizing this acceleration significantly increased the blast overpressure necessary to create similar righting time deficits immediately after blast loading. Together, these data show that significant head accelerations can occur with blast

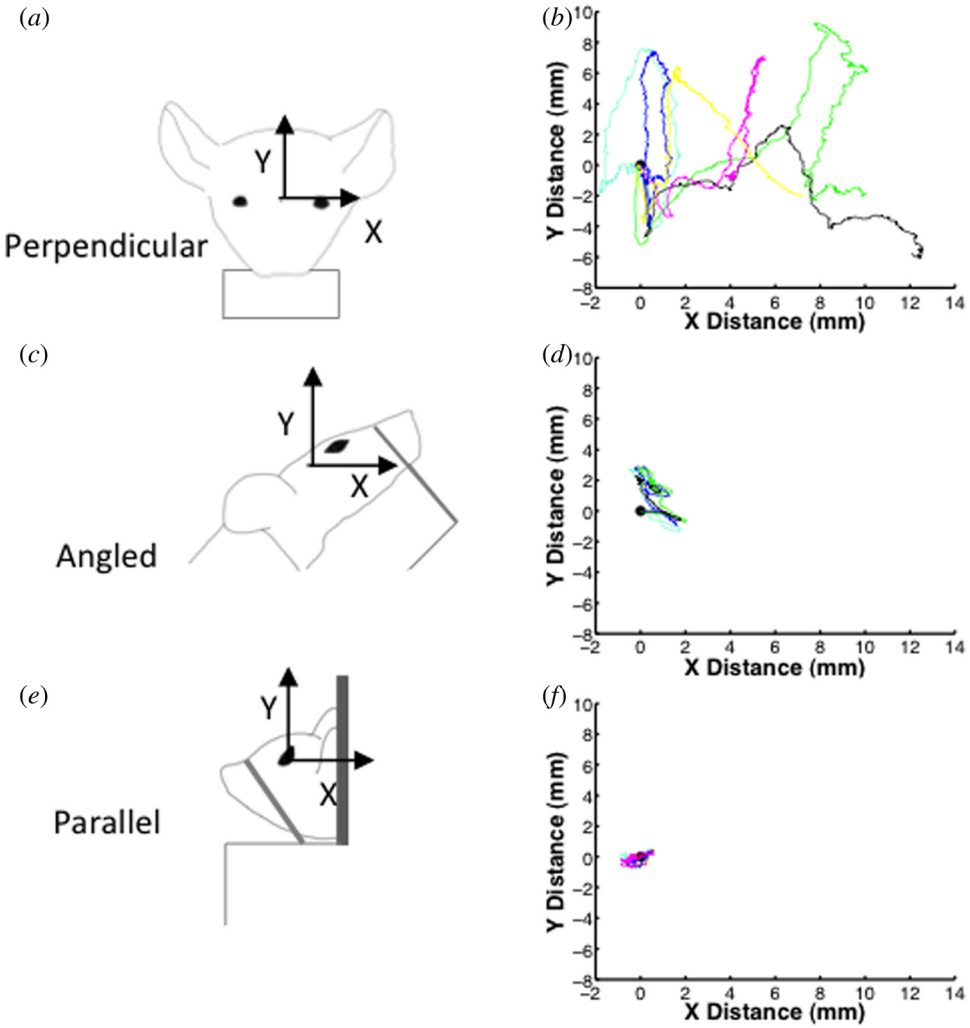

Fig. 4 Displacement that occurs during each blast event for the perpendicular ((*b*); $n = 6$), angled ((*d*); $n = 4$), and parallel ((*f*); $n = 4$) orientations. Different color traces represent different trials in the same orientation. Schematic diagrams ((*a*), (*c*), and (*e*)) of the mouse head position, extracted from high speed video recordings, prior to blast exposure. (*b*) Vertical (*y*) movement of the head in the perpendicular configuration is consistent during the first phase of motion (initial position denoted by dot) and shows more variability in lateral movement across tests. (*d*) Angled positioning of the head relative to the incoming blast wave reduced motion substantially when compared to the perpendicular position. (*e*) The most limited head motion occurred when the animal was oriented parallel to the shock tube, and the head was supported with a cervical collar. Blast input conditions were kept consistent across tests (average blast overpressure = 215 ± 13 kPa, average blast duration = 0.65 ± 0.04 ms, and average blast impulse = 46 ± 5 kPa·ms). Results are reported as mean ± SD.

exposure in a mouse model of TBI, and this feature must be either considered or minimized when interpreting the brain injuries that appear in models of bTBI.

bTBI models are increasing in number and include both rodent and higher order species. Existing work in mice shows that the exposure of either the whole body or only the head to the shockwave can cause a markedly different physiological response, a differential release of stress markers, and a significant difference in neurological impairment [28–30]. In our work, we were careful to shield the torso from the shockwave. Therefore, our model focuses the effects of the shockwave on the brain and minimized the effects to other organs. Moreover, our model uses peak pressures that are often well above previous studies, but the duration of these pressures is well below nearly all previous reports in rodents. Therefore, the average impulse loading used in our shock tube places it within the range of prior work [7,30–36]. In past studies, rodent model characterization has concentrated on measuring the transfer of the external blast wave to the pressure within the brain parenchyma, and several features emerged as important: the orientation of the animal to the incident wave, the position of the animal within or outside the shock tube, and even the methodology used to measure the intracranial pressure transients [16,18,36]. Our current work extends this past work by providing systematic measures of head accelerations when the orientation of the blast wave is altered relative to the axis of the animal. In general, our findings on the potential importance of head acceleration in models of blast injury are consistent with past findings from Goldstein et al. [19] and Svetlov et al. [20].

Our results and other recent studies together show one must be cautious when interpreting the mechanisms of brain injury that are sustained in current rodent models of bTBI. Many studies consider pressure transients within the brain as a primary injury mechanism for blast injury. Svetlov and colleagues [20] were the first to point out the complex dynamics of the blast wave and the role that the

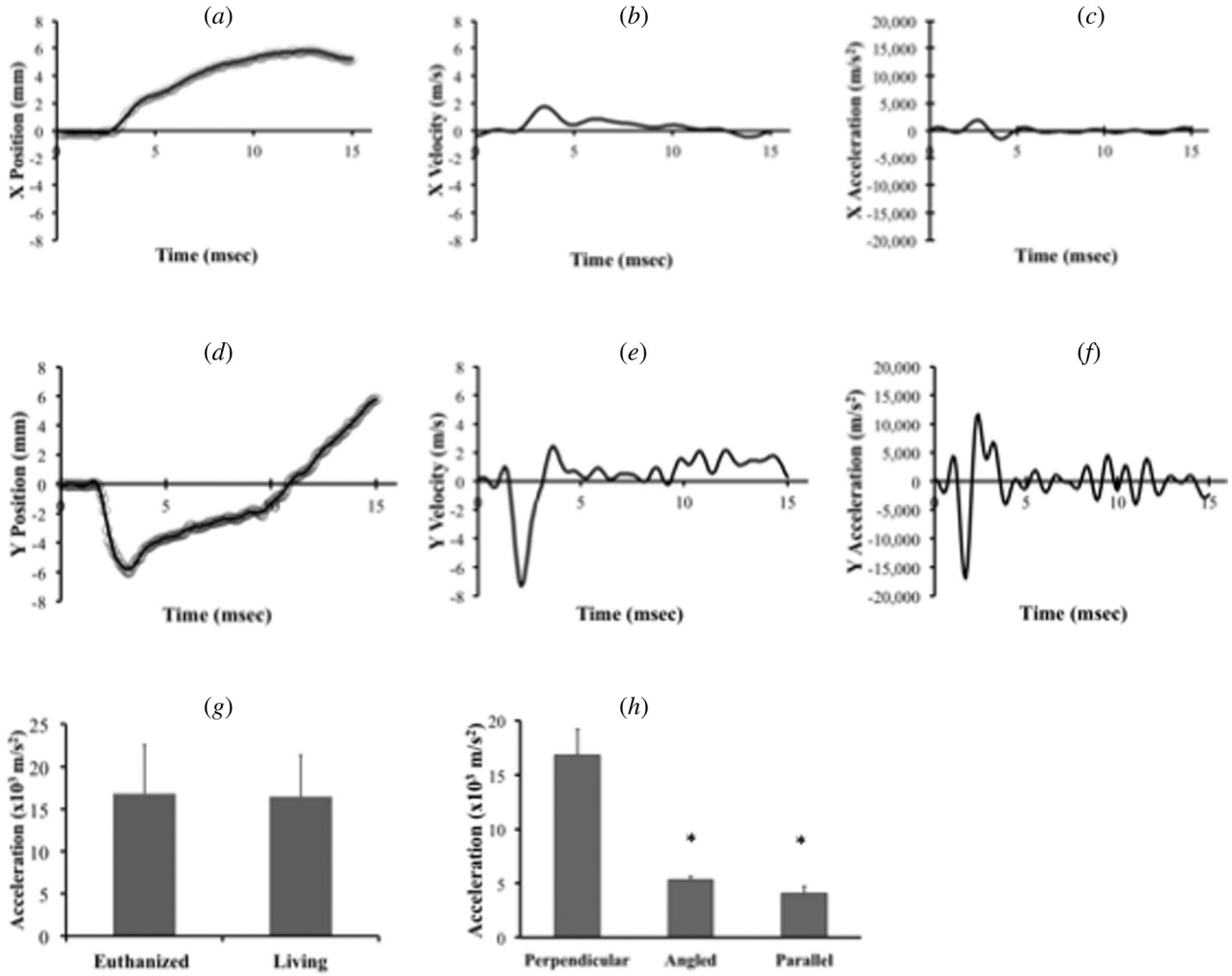

Fig. 5 Horizontal ((*a*)–(*c*)) and vertical ((*d*)-(*f*)) components of motion resulting from a blast exposure with the mouse aligned perpendicular to the incoming blast wave, and positioned along the periphery of the shock tube (Fig. 1(*b*)). Position graphs ((*a*) and (*d*)) display both the original data (black circles) and filtered output (black line). Velocities ((*b*) and (*e*)) and accelerations ((*c*) and (*f*)) were calculated from the filtered displacement data. Peak resultant accelerations were significantly higher when the animal was placed perpendicular to the direction of the blast wave (*g*). SDs are indicated (*g*). Asterisk (*) indicates a significant difference ($p < 0.05$) based on posthoc testing between the perpendicular condition and angled and parallel groups. The angled and parallel groups were not significantly different from each other.

gas jet may play in both rapid head motion and compression of the rodent skull. Moreover, a recent study by Sundaramurthy [5] examined the potential interplay between the primary blast wave and subsequent blast wind at different points along the shock tube axis, demonstrating that animal motion can be minimized at one point within a specific shock tube design. Our measured pressure profiles along the tube length and immediately outside the tube exit showed that our loading was composed of a shock wavefront and a gas fluid flow. Measures of the intracranial pressure in other studies [34,37–39] often show a reflection peak followed by a transient similar to the applied blast exposure, and preliminary measurements in our shock tube show similar changes [40]. We have not yet examined how the diffraction effects of the wave at the head surface, as outlined by Sundaramurthy [5], play a role in the intracranial pressure (ICP) changes. Moreover, we do not have precise measurements of skull deflection that can occur following blast exposure [11]. However, we did not find a position either inside or outside the tube where the gas flow effects were minimal in our shock tube design. Therefore, we expect that both blast overpressure and head accelerations could contribute to the injury response in the mouse after blast exposure.

Measures of the head accelerations in our shock tube tests can be used to estimate the relative significance of the rotational accelerations. Approximations of rotational acceleration occurring in the perpendicular configuration tests (distance from head center to midcervical spine: 1.9 cm; peak rotational acceleration = ~800 krad/s^2; scaled human rotational acceleration ~ 10 krad/s^2) place the murine model accelerations slightly above the range estimated for concussion in humans derived from field studies, computational models, and scaling of acceleration-based animal models [41–43]. The relative magnitude of acceleration we observed in mice is roughly similar to the resultant head accelerations observed in porcine testing using a similar blast overpressure level [14]. Neither the scaled accelerations in our mouse model nor the porcine accelerations were sufficient to cause any mass lesions or hemorrhagic damage in the brain. In some past reports, blast loading in rodents can cause subarachnoid hemorrhage and brainstem lesions [44,45]. In studies where the head motion was minimized, though, our current work and past studies [11,19,21] show that the effects of primary blast loading will leave relatively little macroscopic vascular damage. The mechanism leading to bleeding along the brain surface or in the brainstem region is not described in past studies [44,45], and we speculate it could occur from the compression of the head observed in the Svetlov study, the complex interplay between the blast exposure, thoracic pressure and intracranial pressure noted in the Sundaramurthy study. Overall,

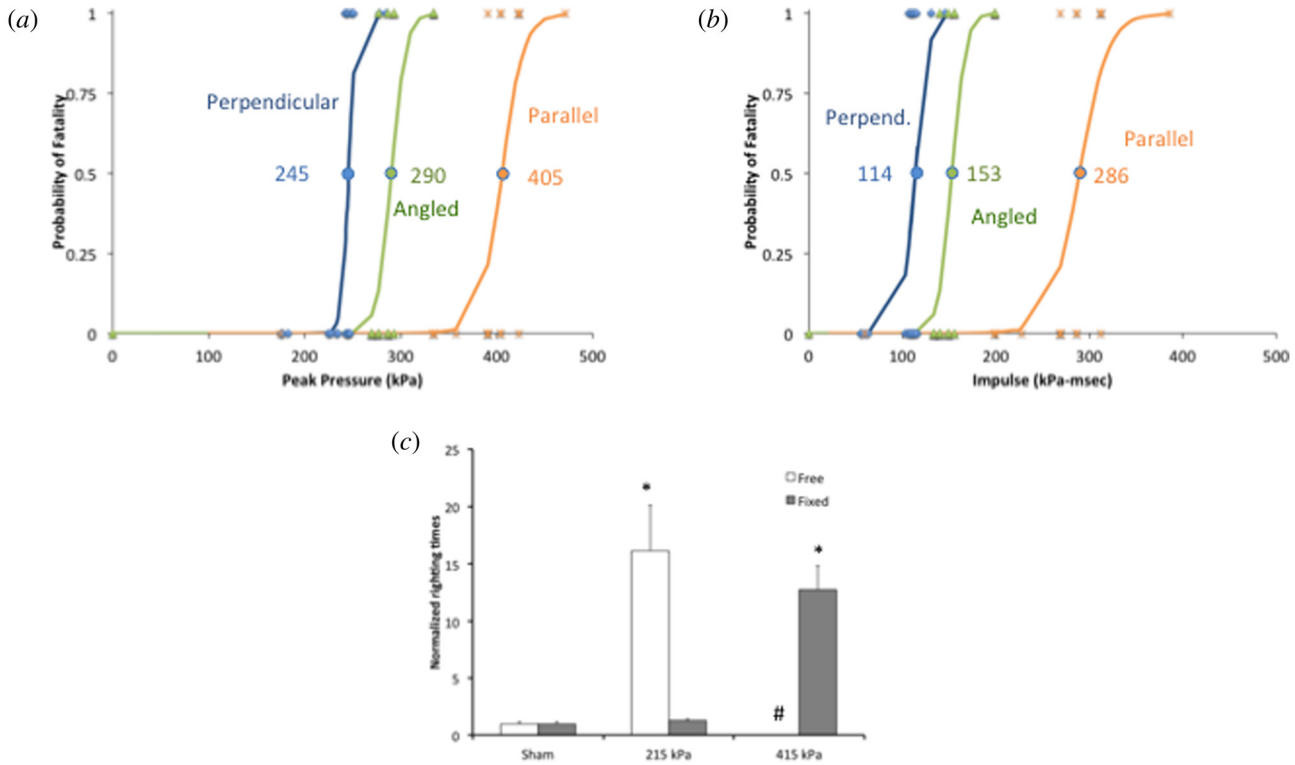

Fig. 6 Induced head acceleration influences survival and immediate neurological impairment following blast exposure. (*a*) Fatality data (0 = survive; 1 = fatal) for two biomechanical scenarios—(1) a blast wave transmitting an intracranial pressure change and a significant head acceleration (perpendicular orientation), and (2) a blast wave that only transmitted an intracranial pressure change, with reduced head acceleration (angled and parallel orientations). Logistic regression analysis on the survival data showed that the lowest survival thresholds appeared when the head was allowed to move during the blast event ((*a*) and (*b*)). Significant differences in the blast overpressure and impulse for 50% survival probability appeared across all three orientations. Numbers correspond to the pressure/impulse associated with 50% fatality in each configuration. (*c*) Righting times normalized to sham for the perpendicular and parallel orientations. For equivalent blast overpressures that caused only transient impairment (215 ± 13 kPa), restraining the head led to a complete loss of functional impairment after blast exposure. However, it was possible to cause a significant righting time deficit even when the head was constrained, although the necessary blast overpressure levels (415 ± 41 kPa) were significantly higher than the unrestrained head motion tests. (*N* = 10–13 animals/group; average ± standard error shown).

the collective results from the current study and past investigations point toward the value of studying how the applied blast exposure can cause varying levels of head motions and how the presence/absence of these motions will affect both the macroscopic/microscopic injury patterns and the functional impairment (e.g., righting time) caused by the blast loading.

We evaluated different approaches to reduce these accelerations. We considered moving the animal to a position outside the primary airflow path to limit the head acceleration caused by the gas jet from the tube [11] but were concerned that the repositioning would limit the magnitude of the shock wave exposure possible in our model. Alternatively, we also considered moving the animal into the shock tube to minimize head motion [5], but the size of the animal holder relative to the shock tube diameter would significantly magnify the loading on the animal because of confinement problems. Next, we evaluated the effectiveness of different padding materials underneath the animal, but saw no measurable change in the resulting head motions. After testing simple approaches to restrain the head, we found a combination design using a custom cervical collar and an unobtrusive snout constraint was much more effective in controlling head motions during blast and preventing any translation of the animal in the holder.

The impact of our efforts to reduce head motion during blast was twofold: the survivability threshold increased significantly and the threshold for the impairment in righting time also increased. Our result showing that we eliminated righting time impairment completely by significantly reducing head motions is similar to a recent study showing that neurobehavior deficits after blast are eliminated when head movement is minimized during blast [19]. We recognize that our efforts to minimize head motion also required us to change the direction of the incoming blast wave from perpendicular to parallel to the mouse's long-axis, primarily because we could more effectively limit head motion in this configuration. We chose to test more completely the parallel configuration because it provided the most effective head immobilization, therefore providing an experimental method to study the effect of primary blast exposure without the complications of induced accelerations. Similar head immobilization occurred with the angled orientation, but the increased neck flexion led to brainstem-based fatalities at higher pressures. These data point us toward future studies where we will examine if blast exposure in mice—where head motion is reduced—will lead to measurable neurobehavior deficits.

In conclusion, although our findings highlight the possibility that significant accelerations may occur in rodent models of bTBI, we also show that it is possible to limit this complicating experimental factor. We expect these findings will provide an additional approach for understanding the precise mechanistic differences for blast TBI that are unique from the impact/acceleration-based mechanisms of TBI. Developing more information on both common and unique mechanisms across these different phases of blast-induced TBI will inevitably shed more light on how different diagnostic and treatment strategies can be optimized to detect and treat these important forms of bTBI.

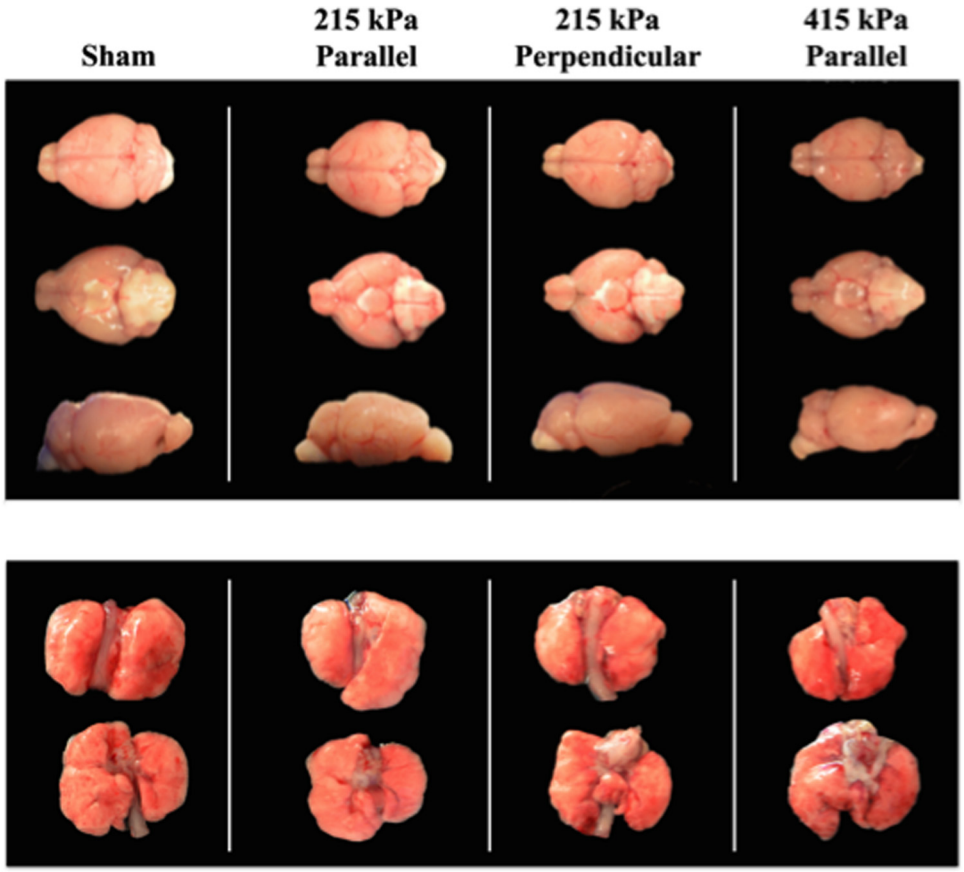

Fig. 7 Brain injury patterns in surviving animals. Following blast exposure in either the perpendicular or parallel orientation, animals showed no signs of bleeding along the surface of the brain. Moreover, there was no sign of subarachnoid hemorrhage or primary brainstem damage. There was no apparent difference in overt changes to the brain following two different levels of blast exposure (parallel orientation). Images of the lungs showed no macroscopic signs of hemorrhage. All samples were collected 15 min following blast exposure.

Acknowledgment

Funding for this project was provided by the Department of the Army Grant No. W911F-10-1-0526. We would also like to thank Edward W. Vogel III, Christopher D. Hue, and Gwen B. Effgen from Columbia University for their input and help with high speed video acquisition. Finally, we would like to thank Anthony Choo, Rosalind Mott, and Tanya Merdiushev for their input to the project.

References

[1] Orman, J. A., Geyer, D., Jones, J., Schneider, E. B., Grafman, J., Pugh, M. J., and Dubose, J., 2012, "Epidemiology of Moderate-to-Severe Penetrating Versus Closed Traumatic Brain Injury in the Iraq and Afghanistan Wars," J. Trauma Acute Care Surg., **73**(6 Suppl 5), pp. S496–S502.

[2] Taniellan, T., and Jaycox, L. H., 2008, "Invisible Wounds of War: Psychological and Cognitive Injuries, Their Consequencesm and Services to Assist Recovery," Report No. MG-720-CCF.

[3] Bass, C. R., Panzer, M. B., Rafaels, K. A., Wood, G., Shridharani, J., and Capehart, B., 2012, "Brain Injuries From Blast," Ann. Biomed. Eng., **40**(1), pp. 185–202.

[4] Cernak, I., Wang, Z., Jiang, J., Bian, X., and Savic, J., 2001, "Ultrastructural and Functional Characteristics of Blast Injury-Induced Neurotrauma," J. Trauma, **50**(4), pp. 695–706.

[5] Sundaramurthy, A., Alai, A., Ganpule, S., Holmberg, A., Plougonven, E., and Chandra, N., 2012, "Blast-Induced Biomechanical Loading of the Rat: An Experimental and Anatomically Accurate Computational Blast Injury Model," J. Neurotrauma, **29**(13), pp. 2352–2364.

[6] Wang, Y., Wei, Y., Oguntayo, S., Wilkins, W., Arun, P., Valiyaveettil, M., Song, J., Long, J. B., and Nambiar, M. P., 2011, "Tightly Coupled Repetitive Blast-Induced Traumatic Brain Injury: Development and Characterization in Mice," J. Neurotrauma, **28**(10), pp. 2171–2183.

[7] Long, J. B., Bentley, T. L., Wessner, K. A., Cerone, C., Sweeney, S., and Bauman, R. A., 2009, "Blast Overpressure in Rats: Recreating a Battlefield Injury in the Laboratory," J. Neurotrauma, **26**(6), pp. 827–840.

[8] Baalman, K., Cotton, J., Rasband, N., and Rasband, M., 2012, "Blast Wave Exposure Impairs Memory and Decreases Axon Initial Segment Length," J. Neurotrauma, **30**(9), pp. 741–751.

[9] Shah, A. S., Stemper, B. D., and Pintar, F. A., 2012, "Development and Characterization of an Open-Ended Shock Tube for the Study of Blast mTBI," Biomed. Sci. Instrum., **48**, pp. 393–400.

[10] Ahlers, S. T., Vasserman-Stokes, E., Shaughness, M. C., Hall, A. A., Shear, D. A., Chavko, M., McCarron, R. M., and Stone, J. R., 2012, "Assessment of the Effects of Acute and Repeated Exposure to Blast Overpressure in Rodents: Toward a Greater Understanding of Blast and the Potential Ramifications for Injury in Humans Exposed to Blast," Front. Neurol., **3**, p. 00032.

[11] Svetlov, S. I., Prima, V., Glushakova, O., Svetlov, A., Kirk, D. R., Gutierrez, H., Serebruany, V. L., Curley, K. C., Wang, K. K., and Hayes, R. L., 2012, "Neuro-Glial and Systemic Mechanisms of Pathological Responses in Rat Models of Primary Blast Overpressure Compared to "Composite" Blast," Front. Neurol., **3**, p. 00015.

[12] Effgen, G. B., Hue, C. D., Vogel, III, E. W., Panzer, M. B., Meaney, D. F., Bass, C. R., and Morrison, III, B., 2012, "A Multiscale Approach to Blast Neurotrauma Modeling: Part II: Methodology for Inducing Blast Injury to In Vitro Models," Front. Neurol., **3**, p. 00023.

[13] Arun, P., Abu-Taleb, R., Valiyaveettil, M., Wang, Y., Long, J. B., and Nambiar, M. P., 2012, "Transient Changes in Neuronal Cell Membrane Permeability After Blast Exposure," Neuroreport, **23**(6), pp. 342–346.

[14] Shridharani, J. K., Wood, G. W., Panzer, M. B., Capehart, B. P., Nyein, M. K., Radovitzky, R. A., and Bass, C. R., 2012, "Porcine Head Response to Blast," Front. Neurol., **3**, p. 00070.

[15] Liu, H., Kang, J., Chen, J., Li, G., Li, X., and Wang, J., 2012, "Intracranial Pressure Response to Non-Penetrating Ballistic Impact: An Experimental Study Using a Pig Physical Head Model and Live Pigs," Int. J. Med. Sci., **9**(8), pp. 655–664.

[16] Dal Cengio Leonardi, A., Keane, N. J., Bir, C. A., Ryan, A. G., Xu, L., and Vandevord, P. J., 2012, "Head Orientation Affects the Intracranial Pressure

Response Resulting From Shock Wave Loading in the Rat," ASME J. Biomech. Eng., **45**(15), pp. 2595–2602.
[17] Ganpule, S., Alai, A., Plougonven, E., and Chandra, N., 2012, "Mechanics of Blast Loading on the Head Models in the Study of Traumatic Brain Injury Using Experimental and Computational Approaches," Biomech. Model Mechanobiol. **12**(3), pp. 511–531.
[18] Leonardi, A. D., Bir, C. A., Ritzel, D. V., and VandeVord, P. J., 2011, "Intracranial Pressure Increases During Exposure to a Shock Wave," J. Neurotrauma, **28**(1), pp. 85–94.
[19] Goldstein, L. E., Fisher, A. M., Tagge, C. A., Zhang, X. L., Velisek, L., Sullivan, J. A., Upreti, C., Kracht, J. M., Ericsson, M., Wojnarowicz, M. W., Goletiani, C. J., Maglakelidze, G. M., Casey, N., Moncaster, J. A., Minaeva, O., Moir, R. D., Nowinski, C. J., Stern, R. A., Cantu, R. C., Geiling, J., Blusztajn, J. K., Wolozin, B. L., Ikezu, T., Stein, T. D., Budson, A. E., Kowall, N. W., Chargin, D., Sharon, A., Saman, S., Hall, G. F., Moss, W. C., Cleveland, R. O., Tanzi, R. E., Stanton, P. K., and McKee, A. C., 2012, "Chronic Traumatic Encephalopathy in Blast-Exposed Military Veterans and a Blast Neurotrauma Mouse Model," Sci. Transl. Med., **4**(134), p. 134ra160.
[20] Svetlov, S. I., Prima, V., Kirk, D. R., Gutierrez, H., Curley, K. C., Hayes, R. L., and Wang, K. K., 2010, "Morphologic and Biochemical Characterization of Brain Injury in a Model of Controlled Blast Overpressure Exposure," J. Trauma, **69**(4), pp. 795–804.
[21] Budde, M. D., Shah, A., McCrea, M., Cullinan, W. E., Pintar, F. A., and Stemper, B. D., 2013, "Primary Blast Traumatic Brain Injury in the Rat: Relating Diffusion Tensor Imaging and Behavior," Front. Neurol., **4**, p. 00154.
[22] Panzer, M. B., Matthews, K. A., Yu, A. W., Morrison, III, B., Meaney, D. F., and Bass, C. R., 2012, "A Multiscale Approach to Blast Neurotrauma Modeling: Part I - Development of Novel Test Devices for In Vivo and In Vitro Blast Injury Models," Front. Neurol., **3**, p. 00046.
[23] Hallam, T. M., Floyd, C. L., Folkerts, M. M., Lee, L. L., Gong, Q. Z., Lyeth, B. G., Muizelaar, J. P., and Berman, R. F., 2004, "Comparison of Behavioral Deficits and Acute Neuronal Degeneration in Rat Lateral Fluid Percussion and Weight-Drop Brain Injury Models," J. Neurotrauma, **21**(5), pp. 521–539.
[24] Hayes, R. L., Jenkins, L. W., Lyeth, B. G., Balster, R. L., Robinson, S. E., Clifton, G. L., Stubbins, J. F., and Young, H. F., 1988, "Pretreatment With Phencyclidine, an N-Methyl-D-Aspartate Antagonist, Attenuates Long-Term Behavioral Deficits in the Rat Produced by Traumatic Brain Injury," J. Neurotrauma, **5**(4), pp. 259–274.
[25] Kane, M. J., Angoa-Perez, M., Briggs, D. I., Viano, D. C., Kreipke, C. W., and Kuhn, D. M., 2012, "A Mouse Model of Human Repetitive Mild Traumatic Brain Injury," J. Neurosci. Methods, **203**(1), pp. 41–49.
[26] Friedlander, F. G., 1946, "The Diffraction of Sound Pulses; Diffraction by a Semi-Infinite Plane," Proc. R. Soc., London, Sec. A, **186**(1006), pp. 322–344.
[27] Bass, C. R., Rafaels, K. A., and Salzar, R. S., 2008, "Pulmonary Injury Risk Assessment for Short-Duration Blasts," J. Trauma, **65**(3), pp. 604–615.
[28] Valiyaveettil, M., Alamneh, Y. A., Miller, S. A., Hammamieh, R., Arun, P., Wang, Y., Wei, Y., Oguntayo, S., Long, J. B., and Nambiar, M. P., 2013, "Modulation of Cholinergic Pathways and Inflammatory Mediators in Blast-Induced Traumatic Brain Injury," Chem. Biol. Interact. **203**(1), pp. 371–375.
[29] Arun, P., Oguntayo, S., Alamneh, Y., Honnold, C., Wang, Y., Valiyaveettil, M., Long, J. B., and Nambiar, M. P., 2012, "Rapid Release of Tissue Enzymes Into Blood After Blast Exposure: Potential Use as Biological Dosimeters," PloS one, **7**(4), p. e33798.
[30] Koliatsos, V. E., Cernak, I., Xu, L., Song, Y., Savonenko, A., Crain, B. J., Eberhart, C. G., Frangakis, C. E., Melnikova, T., Kim, H., and Lee, D., 2011, "A Mouse Model of Blast Injury to Brain: Initial Pathological, Neuropathological, and Behavioral Characterization," J. Neuropathol. Exp. Neurol., **70**(5), pp. 399–416.
[31] Risling, M., Plantman, S., Angeria, M., Rostami, E., Bellander, B. M., Kirkegaard, M., Arborelius, U., and Davidsson, J., 2011, "Mechanisms of Blast Induced Brain Injuries, Experimental Studies in Rats," NeuroImage, **54**(Suppl 1), pp. S89–S97.
[32] Cernak, I., Merkle, A. C., Koliatsos, V. E., Bilik, J. M., Luong, Q. T., Mahota, T. M., Xu, L., Slack, N., Windle, D., and Ahmed, F. A., 2011, "The Pathobiology of Blast Injuries and Blast-Induced Neurotrauma as Identified Using a New Experimental Model of Injury in Mice," Neurobiol. Disease, **41**(2), pp. 538–551.
[33] Vandevord, P. J., Bolander, R., Sajja, V. S., Hay, K., and Bir, C. A., 2012, "Mild Neurotrauma Indicates a Range-Specific Pressure Response to Low Level Shock Wave Exposure," Ann. Biomed. Eng., **40**(1), pp. 227–236.
[34] Bolander, R., Mathie, B., Bir, C., Ritzel, D., and VandeVord, P., 2011, "Skull Flexure as a Contributing Factor in the Mechanism of Injury in the Rat When Exposed to a Shock Wave," Ann. Biomed. Eng., **39**(10), pp. 2550–2559.
[35] Saljo, A., Bolouri, H., Mayorga, M., Svensson, B., and Hamberger, A., 2010, "Low-Level Blast Raises Intracranial Pressure and Impairs Cognitive Function in Rats: Prophylaxis With Processed Cereal Feed," J. Neurotrauma, **27**(2), pp. 383–389.
[36] Chavko, M., Watanabe, T., Adeeb, S., Lankasky, J., Ahlers, S. T., and McCarron, R. M., 2011, "Relationship Between Orientation to a Blast and Pressure Wave Propagation Inside the Rat Brain," J. Neurosci. Methods, **195**(1), pp. 61–66.
[37] Chavko, M., Koller, W. A., Prusaczyk, W. K., and McCarron, R. M., 2007, "Measurement of Blast Wave by a Miniature Fiber Optic Pressure Transducer in the Rat Brain," J. Neurosci. Methods, **159**(2), pp. 277–281.
[38] Dal Cengio Leonardi, A., Keane, N. J., Hay, K., Ryan, A. G., Bir, C. A., and VandeVord, P. J., 2013, "Methodology and Evaluation of Intracranial Pressure Response in Rats Exposed to Complex Shock Waves," Ann. Biomed. Eng., **41**(12), pp. 2488–2500.
[39] Skotak, M., Wang, F., Alai, A., Holmberg, A., Harris, S., Switzer, R. C., and Chandra, N., 2013, "Rat Injury Model Under Controlled Field-Relevant Primary Blast Conditions: Acute Response to a Wide Range of Peak Overpressures," J. Neurotrauma, **30**(13), pp. 1147–1160.
[40] Yu, A. W., Wang, H., Matthews, K. A., Rafaels, K. A., Laskowitz, D. T., Gullotti, D., Meaney, D. F., Morrison, III, B., and Bass, C. R., 2012, "Mouse Lethality Risk and Intracranial Pressure During Exposure to Blast," Biomedical Engineering Society Annual Meeting, BMES, Atlanta, GA, Oct. 24–27.
[41] Pellman, E. J., Viano, D. C., Tucker, A. M., and Casson, I. R., 2003, "Concussion in Professional Football: Location and Direction of Helmet Impacts-Part 2," Neurosurgery, **53**(6), pp. 1328–1340; discussion 1340–1321.
[42] Zhang, L., Yang, K. H., and King, A. I., 2004, "A Proposed Injury Threshold for Mild Traumatic Brain Injury," ASME J. Biomech. Eng., **126**(2), pp. 226–236.
[43] Meaney, D. F., Smith, D. H., Shreiber, D. I., Bain, A. C., Miller, R. T., Ross, D. T., and Gennarelli, T. A., 1995, "Biomechanical Analysis of Experimental Diffuse Axonal Injury," J. Neurotrauma, **12**(4), pp. 689–694.
[44] Kuehn, R., Simard, P. F., Driscoll, I., Keledjian, K., Ivanova, S., Tosun, C., Williams, A., Bochicchio, G., Gerzanich, V., and Simard, J. M., 2011, "Rodent Model of Direct Cranial Blast Injury," J. Neurotrauma, **28**(10), pp. 2155–2169.
[45] Nakagawa, A., Fujimura, M., Kato, K., Okuyama, H., Hashimoto, T., Takayama, K., and Tominaga, T., 2008, "Shock Wave-Induced Brain Injury in Rat: Novel Traumatic Brain Injury Animal Model," Acta Neurochir. Suppl., **102**, pp. 421–424.